Development 133, 4527-4537 (2006) doi:10.1242/dev.02651

CPEB controls oocyte growth and follicle development in the mouse

Waldemar J. Racki and Joel D. Richter*

CPEB is a sequence-specific RNA-binding protein that regulates polyadenylation-induced translation. In *Cpeb* knockout mice, meiotic progression is disrupted at pachytene due to inhibited translation of synaptonemal complex protein mRNAs. To assess the function of CPEB after pachytene, we used the zona pellucida 3 (*Zp3*) promoter to generate transgenic mice expressing siRNA that induce the destruction of *Cpeb* mRNA. Oocytes from these animals do not develop normally; they undergo parthenogenetic cell division in the ovary, exhibit abnormal polar bodies, are detached from the cumulus granulosa cell layer, and display spindle and nuclear anomalies. In addition, many follicles contain apoptotic granulosa cells. CPEB binds several oocyte mRNAs, including *Smad1*, *Smad5*, spindlin, *Bub1b*, *Mos*, *H1foo, Obox1*, *Dnmt1o*, *TiParp*, *Trim61* and *Gdf9*, a well described oocyte-expressed growth factor that is necessary for follicle development. In *Cpeb* knockdown oocytes, *Gdf9* RNA has a shortened poly(A) tail and reduced expression. These data indicate that CPEB controls the expression of *Gdf9* mRNA, which in turn is necessary for oocyte-follicle development. Finally, several phenotypes, i.e. progressive oocyte loss and infertility, elicited by the knockdown of CPEB in oocytes resemble those of the human premature ovarian failure syndrome.

KEY WORDS: CPEB, Oogenesis, Translational control, Polyadenylation, Mouse

INTRODUCTION

Early animal development is programmed by maternally inherited mRNAs that are synthesized during oogenesis (Wickens et al., 2000; Richter, 2000). These mRNAs are translated during oocyte maturation, when the cell enters the meiotic divisions, and during embryogenesis. Several dormant mRNAs in oocytes have short poly(A) tails, and when these tails are subsequently elongated, translation ensues. While probably all vertebrate oocytes contain maternal mRNA that is regulated by polyadenylation, most molecular details have been elucidated in *Xenopus*. mRNAs that undergo polyadenylation-induced translation contain two *cis*-acting sequences in the 3′ UTR: the cytoplasmic polyadenylation element (CPE) and the polyadenylation hexanucleotide AAUAAA. The CPE is bound by CPEB and the AAUAAA interacts with cleavage and polyadenylation specificity factor (CPSF) (Mendez and Richter, 2001). In response to progesterone signaling, the kinase Aurora A is activated by dissociating from glycogen synthase kinase 3 (GSK-3) (Sarkissian et al., 2004), and phosphorylates CPEB S174, which in turn activates the cytoplasmic polyadenylation machinery (Mendez et al., 2000a; Mendez et al., 2000b). This machinery includes not only CPEB and CPSF, but also Symplekin, which acts as a molecular scaffold, and GLD2, a poly(A) polymerase (Barnard et al., 2004). CPEB S174 phosphorylation stimulates the activity of GLD2, although the mechanism by which this is accomplished is unclear. Polyadenylation controls translation through maskin, a CPEB-associated protein (Stebbins-Boaz et al., 1999; Barnard et al., 2005). Maskin also binds the cap-binding factor eIF4E, and this interaction prevents the assembly of the eIF4F (eIF4E, eIF4G, eIF4A) initiation complex. Polyadenylation, however, causes the dissociation of maskin from eIF4E, thereby allowing the translation initiation to proceed (Cao and Richter, 2002; Richter and Sonenberg, 2005).

Program in Molecular Medicine, University of Massachusetts Medical School, Worcester, MA 01605, USA.

*Author for correspondence (e-mail: joel.richter@umassmed.edu)

Accepted 18 September 2006

In the maturing mouse oocytes, CPE-dependent polyadenylation also induces translation (Vassalli et al., 1989; Huarte et al., 1992; Gebauer et al., 1994; Oh et al., 2000), which is controlled by CPEB (Tay et al., 2000). A *Cpeb* knockout mouse (KO) was generated with the expectation that oocyte maturation would not proceed normally (Tay and Richter, 2001). Surprisingly, however, female mice contained no ovary; embryonic day (E) 18.5 female embryos contained ovaries but were mostly devoid of oocytes. E16.5 embryo ovaries contained oocytes, but their chromatin was morphologically abnormal and their development was arrested at pachytene, a stage when the synaptonemal complex promotes homologous recombination. In the KO mice, synaptonemal complex proteins SCP1 and SCP3 (SYCP1 and SYCP3 – Mouse Genome Informatics) were not synthesized, and the CPE-containing RNAs that encoded them were not polyadenylated (Tay and Richter, 2001). Thus, CPEB controls an earlier stage of meiosis than previously suspected. Spermatogenesis was also disrupted at pachytene in CPEB KO male mice, demonstrating that CPEB is a general regulator of meiosis.

Further investigations revealed that mouse oocyte CPEB T171 (equivalent to S174 in *Xenopus*) was phosphorylated at E16.5 (pachytene), underwent protein phosphatase 1 (PP1)-catalyzed dephosphorylation at E18.5, and again became phosphorylated during oocyte maturation (Tay et al., 2003). These results suggested that CPEB-mediated polyadenylation would probably next take place during maturation, when it promotes the translation of several mRNAs, including *Mos* and cyclin B1 (Gebauer et al., 1994; Tay et al., 2000; Hodgman et al., 2001). The translation of *Mos* mRNA is particularly important for mouse development. MOS is a protein kinase that activates the MAP kinase cascade, which culminates in the activation of maturation promoting factor (MPF), a heterodimer of CDC2 and cyclin B1 that induces maturation; MOS thus has a mitogenic activity. MOS has a second activity; it is a component of the cytostatic factor (CSF) complex that prevents oocyte development beyond meiosis II (MII) until fertilization stimulates the resumption of cell division (O'Keefe et al., 1989; Sagata, 1997; Gebauer and Richter, 1997; Tunquist and Maller, 2003). In *Xenopus*

oocytes, MOS has both these activities, but in mouse oocytes it has retained only the CSF activity. Thus, oocytes derived from *Mos* knockout mice often fail to arrest at MII and undergo a high rate of parthenogenetic activation (Colledge et al., 1994; Hashimoto et al., 1994; Choi et al., 1996).

Because *Mos* mRNA translation is regulated by cytoplasmic polyadenylation (Gebauer et al., 1994), we hypothesized that oocytes lacking CPEB would have reduced CSF activity and consequently undergo parthenogenetic activation. However, an investigation of this possibility required that oocytes contain CPEB at pachytene but not beyond this stage, thus obviating the use of the *Cpeb* KO mice. Consequently, we sought to destroy *Cpeb* mRNA after pachytene by generating transgenic (TG) mice expressing siRNA under the control of the zona pellucida 3 (*Zp3*) promoter. The *Zp3* promoter is expressed in growing dictyate stage oocytes at the end of prophase I (Epifano et al., 1995).

An analysis of several TG mouse lines demonstrated that *Cpeb* RNA was indeed substantially destroyed by the siRNA. While ovaries from pre-pubertal TG females were morphologically identical to those of wild-type animals, at puberty (6-8 weeks) and in older animals, a number of oocyte and ovarian abnormalities were observed: these included premature oocyte maturation and increased oocyte atresia, parthenogenetic activation, malformed meiotic spindles, precocious follicle activation and granulosa cell apoptosis. Fertility was substantially reduced.

CPEB interacts with a number of CPE-containing RNAs, including those encoding *Mos* and *Gdf9*, a growth factor synthesized in and secreted from oocytes that is important for coordinated oocyte-follicle development (Matzuk et al., 2002; Roy and Matzuk, 2006). In the TG oocytes, both *Mos* and *Gdf9* RNAs had aberrantly short poly(A) tails; GDF9 protein levels were also reduced. Some of the TG oocyte phenotypes resemble those of *Mos* (Colledge et al., 1994; Hashimoto et al., 1994; Choi et al., 1996) and *Gdf9* KO mouse oocytes (Dong et al., 1996; Carabatsos et al., 1998). These results demonstrate that CPEB controls polyadenylation and translation during the dictyate stage, and that this regulation coordinates oocyte/follicle development, which in turn directly affects fertility.

MATERIALS AND METHODS

Plasmid design and mouse breeding

The backbone *Zp3* cassette-SV40 late poly(A), pRL-CMV (Promega) plasmid for the TgZ3GC1 construct is a modified version of pEGFP-N2 (Clontech) and pMoZP3 was kindly provided by Dr Richard Schultz (University of Pennsylvania) and is described in Svoboda et al. (Svoboda et al., 2001) and Stein et al. (Stein et al., 2003). A *Cpeb* dsRNA was constructed by ligating head to head the 645 and 670 nucleotide PCR amplification products encompassing the 612 nucleotides of the *Cpeb* 3′ UTR immediately after the stop codon (plus cloning sites and the loop structure). The 1.3 kb 3′ UTR inverted repeat was subsequently cloned into the pRL-CMV vector (see Fig. 2A). Transgenic mice were generated by pronuclear injection of purified DNA into fertilized embryos harvested from C57BL/6 inbred mice at the UMass Transgenic Animal Core. Transgenic founders were identified by Southern blots and PCR. Seven founder lines of mice, four males and three females, were obtained. These animals were bred to C57BL/6 animals; two males and one female produced offspring. These founders were used to establish three independent lines (i.e. Ln2f, Ln19m and Ln30m) of animals expressing dsRNA targeting CPEB in oocytes. Transgenic F1 males were mated to wild-type littermates and F2 progeny were tested for transgene transmission.

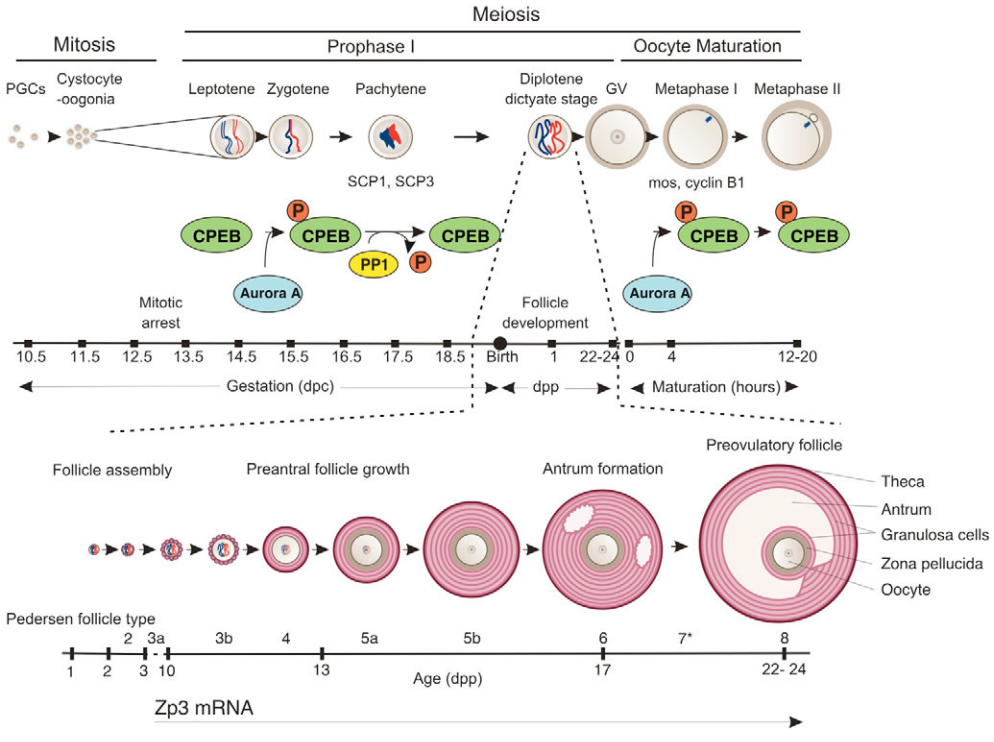

Fig. 1. CPEB activity during oogenesis and oocyte maturation. Migrating and mitotically dividing PGCs begin to populate the genital ridges. Around E12.5-13.5, they arrest and enter meiosis prophase I (~E14.5). Homologous chromosome pairing begins at zygotene [and full synaptonemal complex formation and homologous recombination occurs at pachytene (E17.5)]. At the zygotene to pachytene transition, CPEB is phosphorylated by the kinase Aurora A on T171, which activates the cytoplasmic polyadenylation machinery. Two substrates of CPEB are mRNAs encoding synaptonemal complex proteins 1 and 3 (SCP1 and SCP3), which contain CPEs. In *Cpeb* KO mice, these two proteins are not synthesized and the synaptonemal complex is not formed; the oocytes do not develop beyond pachytene. When the wild-type oocytes progress to diplotene, PP1 dephosphorylates and inactivates CPEB. Oocytes then enter the dictyate stage, which begins before birth and is characterized by oocyte growth and follicle formation. The oocyte synthesizes and secretes the zona pellucida and is surrounded by granulosa cells. In the large preovulatory follicle, the oocyte and granulosa cells reside in the fluid-filled antrum. Upon hormonal signaling, an oocyte enters the meiotic divisions (maturation), which is characterized by germinal vesicle (GV) breakdown, chromosome condensation and polar body extrusion. At this stage, CPEB is re-phosphorylated on T171 by Aurora A, again activating the cytoplasmic polyadenylation machinery that promotes the translation of *Mos* and cyclin B1 RNAs. The *Zp3* promoter becomes active during the dictyate stage.

RNA isolation, RT-PCR, analysis of poly(A), and western blots

RNA from 10 GV stage oocytes as well as ovaries was isolated TRIzol Reagent (Invitrogen) and used for cDNA synthesis. RT-PCR was performed on 2.5- to 5-fold dilutions of first strand synthesis mixture. All primer sequences are listed in Table 1.

The immunoprecipitation of mRNP complexes was performed using ovaries from ten wild-type mice as described (Tenenbaum et al., 2000). The ovaries were homogenized in buffer (100 mmol/l KCl, 5 mmol/l $MgCl_2$, 10 mmol/l HEPES-KOH pH 7.0, 0.5% Nonidet P (NP)-40, 1 mmol/l DTT, 1 mmol/l Na vanadate, 10 mmol/l NaF, 80 mmol/l β-glycero-phosphate, 0.2

Table 1. PCR primers used in this study

Gene/location	Primer	Sequence 5′-3′	Size (nt)
Cpeb1	5′*Bgl*II	GAAGATCTTCACCCACGCTCACCTCCAGATTTATCTTCCAATTACCAGCCAGCGAGAT-TCCAGCTAGTGGAGCTGGCCTT	675
Cpeb1	5′*Bam*HI	GCGGATCCGGTCATATAAGGCACATAAGTGGATTCCAGCTAGTGGAGCTGGCCTT	645
Cpeb1	3′*Xba*I	GCTCTAGAGCCTGTTTTAAGGAGTGTAAAAAGGAA	
Egfp	GFP-f	CTACGGCGTGCAGTGCTTCAGCCGC	473
Egfp	GFP-r	CTCCAGCAGGACCATGTGATCGCGC	
Zp3	CMVfwd	TTCAGGTGGGAGGGTGGGCCATCG	352
Egfp	CMVrev	GAACAGCTCCTCGCCCTTGCTCACC	
Cpeb1	CPEB1#36	AGGCCATCTGGGCTCAGCGGG	560
Cpeb1	CPEB1#43	TCAAGCCTTCGCATTTCCCCTCC	
Mos	MOS fwd	ATCCTGAAAGGAGAGATTGCCACGC	308
Mos	MOS rev	TCGGCTCGATGGAGTCAGCCTAGTG	
Zp3	ZP3 fwd	TAGAGGGTGATGCTGACATCTGTGA	150
Zp3	ZP3 rev	CAGTGACATCAGCTTCATCGGTCAC	
Tuba2	Tub fwd	CCATCCTGAGCAGCTCATCACAGGC	300
Tuba2	Tub rev	GAATTGTAGGGCTCAACCACAGCAG	
Actb	Act fwd	ATTGCTGACAGGATGCAGAAGG	300
Actb	Act rev	AAAGCCATGCCAATGTTGTCTC	
Bub1b	Bub fwd	GGACTTCTCCTACAGTGTTGACCTG	302
Bub1b	Bub rev	CAGACACTGTGGACTTGTCACTGGC	
Dnmt1o	Dnmt fwd	GCTGCTACCAAGGACTAGTGCTCTC	283
Dnmt1o	Dnmt rev	ACTACATCAAGTCTCACTTGCCACC	
Gdf9	GDF9 fwd	CATGGGGGCCACTTCAACAAGC	356
Gdf9	GDF9 frev	ATGCCATCAACAGTTTATTCTTCCGTCACA	
H1Foo	H1Foo fwd	TGAGACAGTACAGGAGACCAAAGTG	213
H1Foo	H1Foo rev	AGACAATAAAAGCTTCAGAATCGCC	
Mater	MATER f	ATGTTGAAGCTGTGCTCTGCGTTCC	279
Mater	MATER r	TTATTTCATTCTTGCTACATCCTCC	
*Msy2**	Msy2 fwd	ACTCAGGAGGGCCAAAGCACCAGCC	268
*Msy2**	Msy2 rev	TTTTTACTGGAGGCTCAGGTGGCAC	
Obox1	OBOX1 f	AGGATGCTCACAATTCAGCTCC	265
Obox1	OBOX1 r	ACTGAATTTCAAACAATCGCACTAC	
RFPL4	RFPL4 f	TAGTTACAGGAAATGCCATTTG	298
RFPL4	RFPL4 r	TTATTTATTCCACAACATCATACAC	
Smad1	SMAD1 f	CAAATCAACTGGCTTCGTGTTTCAG	303
Smad1	SMAD1 r	TACTCGCTGTATAAGAGCAAAGGAG	
Smad4	SMAD4 f	AGAATAATGGAAACAGTGCAGTTGG	265
Smad4	SMAD4 r	GTGTCTGTGGTACAGTCAATGTGTC	
Smad5	SMAD5 F	AAGAATGTGATTACAGAGCGAGTGC	239
Smad5	SMAD5 R	GGCTTTGAGAGCACAATACAG	
Spindlin	Spin fwd	AAAATACTACAAGTAATTGTGGTGG	301
Spindlin	Spin rev	TTTAAGGAAGGATAAGAGTTACATC	
Tiparp	TiPARP f	AAATATACCACAGAAGTCCTTCCGA	316
Tiparp	TiPARP r	ATCAAACAAGCAATGGTAACATGTC	
Trim61	Trim61 f	GCCTTACTTCTACACTGGATATGAC	278
Trim61	Trim61 r	AGGATGTGTCTGTCATTATTGGACG	
Vrk1	Vrk1 fwd	TAGTGCTGTGGAGAACGGAAGTGTG	265
Vrk1	Vrk1 rev	ATGAATAGGCAGAGAAGATGGTTCC	
Zp1	ZP1 fwd	TCTGATACATGCTCTACTACGTGTG	289
Zp1	ZP1 rev	TTGAGTCCATTTAATATCTGATGCC	

**Ybx2* – Mouse Genome Informatics database.

mmol/l PMSF plus protein and RNaze inhibitors [0.2 mmol/l PMSF, 1 μg/ml Pepstatin A, 2 μg/ml Aprotinin, 2 μg/ml Leupeptin, 100 U/ml RNaseOUT (Invitrogen) and 0.2% vanadyl/ribonucleoside complex (GIBCO/BRL)] and frozen at –80°C. The lysate was pre-cleared for 10 minutes at 16,000 ***g*** (4°C). Magnetic beads were washed four times in 1 ml NT2 buffer (50 mmol/l Tris-HCl pH 7.4, 150 mmol/l KCl, 1 mmol/l $MgCl_2$, 0.05% NP-40) and then a final time when supplemented with 5% BSA. The beads were incubated with CPEB antibody or nonspecific IgG at 4°C overnight with tumbling. The beads were washed three times with NT2 buffer and re-suspended in 900 μl NT2 buffer supplemented with protease and RNase inhibitors. One hundred microliters of ovary extract was added, mixed briefly, and immediately centrifuged to collect a 100 μl sample of total RNA. The remaining sample was tumbled overnight at 4°C, then washed six times with cold NT2 buffer; the RNA was isolated using TRIZOL reagent.

To examine poly(A) tail length, we employed poly(U) Sepharose chromatography and thermal elution (Simon et al., 1996; Du and Richter, 2005). Poly(U)-Sepharose (Sigma) was swollen in SB buffer (1 mol/l NaCl, 5 mmol/l Tris-HCl, pH 7.5, 10 mmol/l EDTA, 0.2% SDS), washed three times in EB buffer (90% formamide, 50 mmol/l HEPES, pH 7.5, 10 mmol/l EDTA, 0.2% SDS), and equilibrated in CSB buffer (25% formamide, 0.7 mol/l NaCl, 50 mmol/l Tris-HCl pH 7.5, 1 mmol/l EDTA). The beads (50 μl gravity packed) were mixed with 10 μg total RNA from whole ovaries of 3-week-old mice that was suspended in 50 μl of solution containing 1% SDS and 30 mmol/l EDTA, incubated for 5 minutes at 70°C and then diluted fivefold in CSB buffer. The beads and RNA were mixed with constant inversion for 1 hour at 25°C. The beads were briefly centrifuged, the supernatant was removed, and the beads washed three times with 1 ml each of LSB buffer (25% formamide, 0.1 mol/l NaCl, 50 mmol/l Tris-HCl, pH 7.5, 10 mmol/l EDTA), and then incubated in 0.3 ml LSB at 30°C for 3 minutes, pelleted by brief centrifugation, and the supernatant was removed and saved for analysis. This procedure was repeated for 45°C and 60°C followed by final incubation at 95°C. After each elution, the RNA was extracted and ethanol precipitated.

SDS-PAGE and protein blotting was performed on 10-20 μl of whole single ovary lysate corresponding approximately to 10-20% of the total tissue. The blots were probed with polyclonal CPEB primary antibody at 1:1000, monoclonal GDF9 primary antibody at 1:3000 (courtesy of M. M. Matzuk, Departments of Pathology, Molecular and Cellular Biology and Molecular and Human Genetics, Baylor College of Medicine).

Morphological analysis

Ovaries were washed briefly at room temperature in PBS, pH 7.2, blotted to remove excess liquid and fixed in Bouin's solution for 6-12 hours. The fixed tissue was washed extensively with 70% ethanol and paraffin embedded, sectioned and stained with hematoxylin and eosin. For TUNEL assays, paraffin sections (5 μm) were de-waxed and re-hydrated following standard procedures. The re-hydrated sections were boiled for 10 minutes in 100 mmol/l sodium citrate buffer, pH 6.0, left to cool at room temperature, and washed three times with PBS. The sections then were permeabilized for 2 minutes with 0.1% Triton X-100, 0.1% sodium citrate on ice, followed by three washes with PBS. Labeling was performed using In Situ Cell Death Detection Kit, POD (Roche) according to the manufacturer's instructions.

RESULTS

Generation of transgenic mice

Some salient features of oogenesis and folliculogenesis, as well as the stages during which CPEB has been shown to regulate translation, are depicted in Fig. 1. Primordial germ cells (PGCs) migrating to the genital ridge divide mitotically. In the embryonic ovary, follicle formation is preceded by incomplete synchronous mitotic division leading to the formation of the cystocytes (oocytes with interconnecting cytoplasmic bridges) and enter leptotene of prophase I (Pepling and Spradling, 1998; Pepling and Spradling, 2001). The oocytes contain CPEB at this stage but the protein is not phosphorylated and thus is inactive (Tay et al., 2003). At zygotene to pachytene, Aurora A phosphorylates CPEB T171, which induces the polyadenylation and translation of mRNAs encoding synaptonemal complex proteins 1 and 3 (SCP1, SCP3) (Tay and Richter, 2001). These proteins are essential components of the synaptonemal complex, a structure that promotes homologous recombination. As the oocytes exit pachytene, protein phosphatase 1 (PP1) dephosphorylates and inactivates CPEB. The oocytes then enter the dictyate stage (concomitant with perinatal cytocyst breakdown and primordial follicle formation), which can last from around birth to about 3 weeks; most oocytes, however, remain in the dictyate stage for the entire reproductive period (up 2 years). The oocytes that are activated enter a growth and development phase that takes about 3 weeks to complete; it culminates with re-entry into the meiotic divisions (maturation), when they undergo germinal vesicle breakdown (GVBD) and extrude the first polar body. During maturation, CPEB again is phosphorylated on T171, which promotes polyadenylation and translation of *Mos*, cyclin B1 and other mRNAs (Gebauer et al., 1994; Tay et al., 2000; Hodgman et al., 2001).

During the dictyate stage, the follicle undergoes striking growth and development. The zona pellucida is elaborated, antrum formation occurs, and in preovulatory follicles the oocyte becomes surrounded by several layers of cumulus granulosa cells. The zona pellucida is composed of three proteins, one of which, ZP3, begins to be expressed in growing oocytes (follicle stage 3a) at about day 6 post-partum. Because *Cpeb* KO oocytes do not develop beyond pachytene, we used the *Zp3* promoter to express a palindromic RNA that, when processed by DICER, would generate multiple siRNAs and induce *Cpeb* RNA destruction (Fig. 2A). The 3′ UTR of *Cpeb* was targeted because it had no significant homology with other RNAs, which was not the case with the open reading frame (Mendez and Richter, 2001; Mendez et al., 2002). Consequently, the 612 nucleotide inverted repeat RNA (1301 bases total) was appended to *Gfp* after the stop codon. A vector containing this sequence under the control of the *Zp3* promoter was injected into pronuclear stage eggs from C57BL/6 mice; pups derived from these injected eggs were bred onto C57BL/6.

Three female and four male transgenic founders were analyzed; they appeared normal but two males and one female did not produce offspring. The male infertility was unexpected considering the normal appearance of their reproductive organs, and could be due to insertional inactivation of a gene required for sperm production. The infertile female was sacrificed at 10 months and had hypertrophic ovaries ~4-fold larger than normal with no detectable follicular structure or oocytes; only a single primary stage 3a follicle was detected (see Fig. S1 in the supplementary material). Three lines of CPEB knockdown animals were retained for further analysis. F1 males from all the transgenic lines were fertile and produced offspring with the expected genotypic ratios. Transgenic F1 females from two transgenic lines did not produce offspring after repeated matings for 6 months; females from the other line produced offspring but only up to 4-6 months of age. In two independent experiments per line, single ovaries isolated from three to five F2 TG females contained 61% fewer GV oocytes than wild type (three females used) at 2 months of age, 88% fewer at 12 months of age. However, those few oocytes that were obtained matured in vitro to MII at a rate similar to wild-type oocytes (data not shown).

The F2 offspring from the TG lines and corresponding wild-type littermates were analyzed further; they expressed *Gfp* RNA (Fig. 2B), although a green fluorescent signal was too low to detect. However, in those lines containing *Gfp* RNA, there was almost no detectable *Cpeb* RNA. In line 2f, the efficiency of transgene

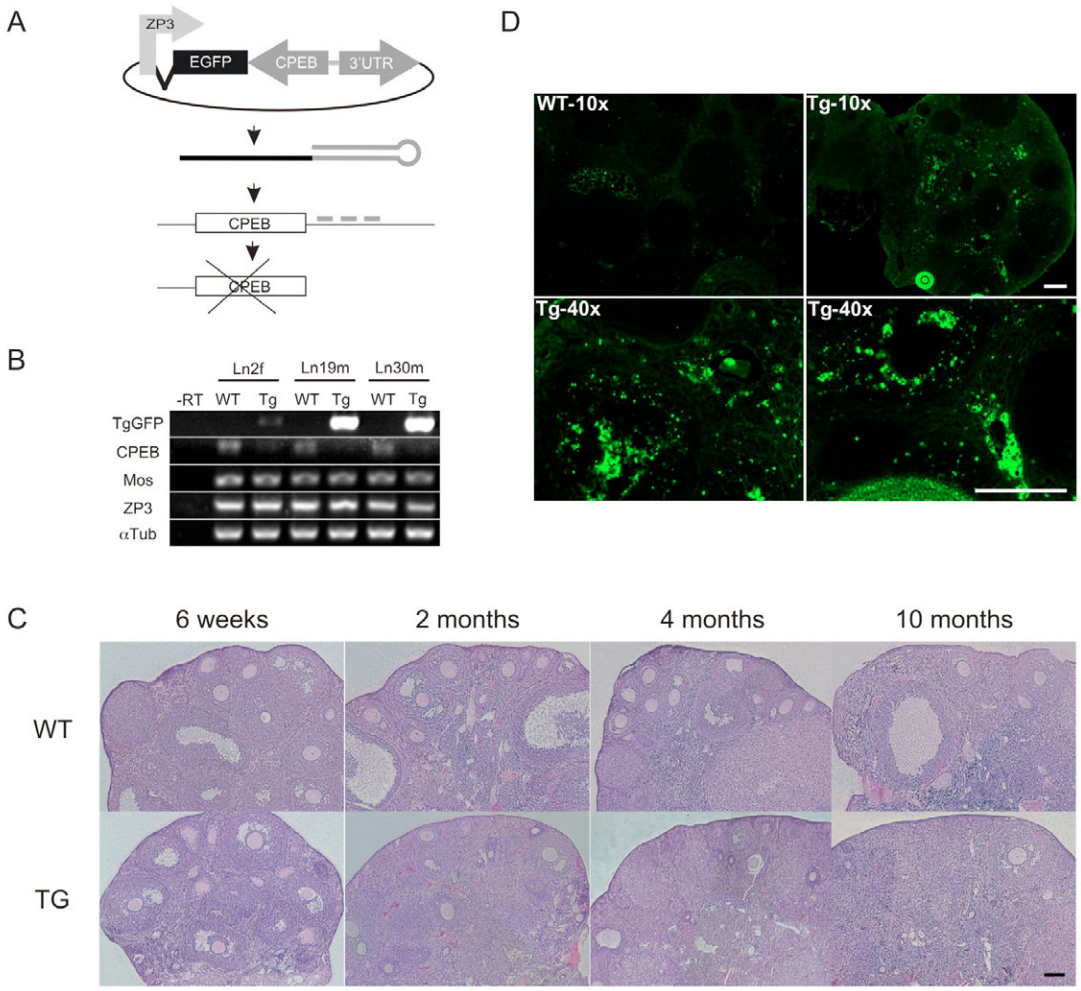

Fig. 2. *Cpeb* knockdown mice. (**A**) Schematic representation of the transgene construct. The *Zp3* promoter was inserted upstream of the *Egfp* open reading frame, which was followed by 1301 bases of the *Cpeb* 3′ UTR in an inverted repeat structure separated by irrelevant loop sequence. The *Cpeb* inverted repeats would form a double-stranded stem and be cleaved by DICER, thus yielding siRNAs that would anneal to the endogenous *Cpeb* 3′ UTR and induce RNA destruction. (**B**) RT-PCR of *Egfp*, *Cpeb*, *Mos*, *Zp3* and α-tubulin mRNAs from ovary extracts derived from 2-month-old animals. (**C**) Ovaries from 8-week, 2-, 4- and 10-month-old animals were fixed, embedded and stained with hematoxylin and eosin. The *Cpeb* knockdown ovaries displayed a progressive decrease in oocyte number and follicles. (**D**) TUNEL labeling of 6-week-old ovaries from wild-type and TG mice. Note that while the wild-type ovary displayed little labeling, the TG ovary was heavily labeled, indicating substantial granulosa cell apoptosis. Scale bars: 100 μm in C,D.

expression was significantly lower compared to the other two lines, which might be expected to produce in a milder phenotype. Indeed, we did observe a range of phenotypes (see Table S1 in supplementary material). The levels of non-targeted *Mos*, *Zp3* and α-tubulin RNAs were all unaffected by the expression of the transgene. We thus conclude that CPEB RNA was efficiently and specifically destroyed by siRNA.

The ovaries from both wild-type and TG animals were examined at intervals from 6 weeks to 10 months (Fig. 2C). While the 6-week-old wild-type and TG ovaries were similar and contained numerous follicles, the 2- and 4-month-old ovaries were strikingly different. At these times, the wild-type ovaries contained numerous follicles but the TG ovaries contained very few. By 10 months, almost no follicles were detected in the TG ovaries. The TG ovary displayed substantial granulosa cell apoptosis, as assessed by a TUNEL assay (Fig. 2D). The wild-type ovary was barely labeled by the TUNEL reagent, indicating that it contained few apoptotic cells.

CPEB controls oocyte development at the dictyate stage

Histological examination of TG ovaries at 6 weeks to 6 months revealed a number of oocyte phenotypes (Fig. 3). Oocytes often underwent precocious maturation (Fig. 3A), formed metaphase chromosomes assembled into multi-polar spindles (Fig. 3A,B, arrows) and improperly lacked the surrounding cumulus granulosa layer (Fig. 3A,B; see also Fig. 4A,C, stars). Other oocytes had chromosomes that were not properly aligned at the metaphase plate and/or underwent anaphase in which some chromosomes did not properly segregate (Fig. 3B, arrow). Some oocytes also had disorganized and mono-polar spindles (Fig. 3C), extruded polar bodies from opposite ends of the cell (Fig. 3D), or contained polar bodies with metaphase chromosomes (Fig. 3E, arrow) or pronucleus-like structures (Fig. 3F, arrow). Other oocytes had improper nuclear envelopes with disorganized chromatin (Fig. 3G, filled arrowheads), contained cytoplasmic structures that resembled nuage or perhaps nucleoli (Fig. 3H,I, empty arrowheads; see also

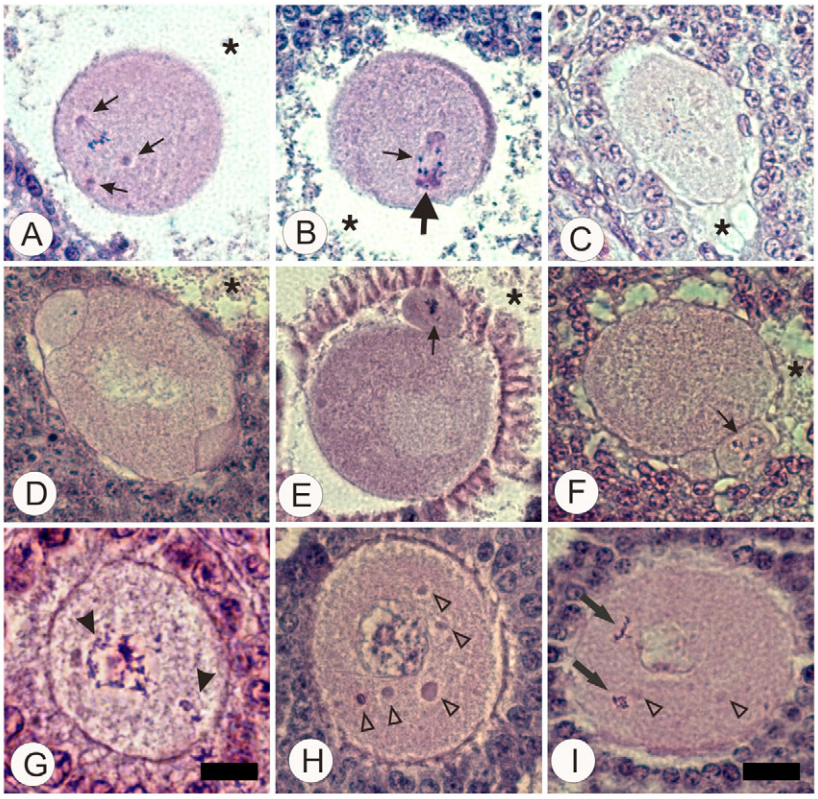

Fig. 3. Post-pachytene knockdown of *Cpeb* results in oocyte abnormalities. Ovaries collected from animals at 2, 4 and 6 months of age were processed for histology as described above. (**A**) An oocyte in a follicle (stage 5-6) that was detached from the cumulus granulosa cells (*) with abnormal and improperly positioned tripolar spindles (arrow). (**B**) The oocyte had a disorganized rosette of chromosomes (arrow) at MI that were spread randomly among three spindle poles (bold arrow). (**C**) This oocyte, enclosed in the asymmetrically developed granulosa cells (one to five layers), in a stage 5a follicle, contained a monopolar spindle; the granulosa cells were also starting to detach. (**D-F**) These pre-antral stage follicles contained MI and MII stage oocytes that displayed apparent granulosa cell apoptosis. (D) This oocyte had improperly extruded polar bodies at opposite sides, and displayed premature antrum formation (*). (E) This oocyte contained a polar body with condensed chromosomes forming a metaphase plate and a spindle. (F) The oocyte, enclosed in a pre-antral follicle, contained a polar body with three pronucleus-like structures. (**G-I**) These oocytes contained poorly structured nuclei and/or nuclear membranes. (G) This stage 3a oocyte lacked a nuclear membrane and contained partially condensed chromatin. Notice the chromatin particles dispersed in the oocyte cytoplasm. (H) This fully developed oocyte lacked normal nuclear membrane and contained several cytoplasmic structures that resemble nuage or perhaps nucleoli (empty arrowheads, also in I). (I) This fully developed oocyte had a disassembled nuclear envelope with condensed chromatin in the cytoplasm. Scale bars: 10 μm in G; 20 μm in all other panels.

Fig. 4I), or contained condensed DNA in the cytoplasm (Fig. 3I, bold arrow). Such anomalies were almost never observed in wild-type ovaries.

Several oocytes showed incipient signs of cell division, or indeed underwent multiple rounds of cell division while in the ovary. Fig. 4A shows an oocyte, having already extruded possibly a second polar body, about to undergo cell division. Fig. 4B-G show oocytes that have undergone parthenogenetic cell division, and, in Fig. 4D-F, up to 15 cells can be detected in each parthenote (notice metaphase cell in D, arrow). Several oocytes also contained multiple fragmented nuclei (Fig. 4G-H, arrows), and appeared to have nuage or perhaps even nucleoli in the cytoplasm (Fig. 4I, empty arrowheads).

We also noted that TG ovaries contained follicles that housed two oocytes (Fig. 5A). The TG ovaries contained a large number of follicles with collapsed oocytes that were aberrantly surrounded by either a single layer of squamous granulosa cells or several layers of highly compact small granulosa cells (Fig. 5B,C). The incidence of this phenotype increased with age, such that by 4 months almost half the follicles resembled those in Fig. 5B,C. Finally, cysts were evident on the TG ovaries (Fig. 5D,E). Four-month-old animals had on average one to three cysts per ovary, which doubled as the animals aged to 12 months. We could detect only a single cyst in ovaries from wild-type animals of the same age (data not shown; however, see Table S1 in the supplementary material).

CPEB control of RNA polyadenylation

To examine the molecular foundation that could be responsible for the phenotypes noted above, we sought to identify oocyte mRNAs that were bound by CPEB. Extracts from wild-type ovaries from 3-week-old mice were mixed with RNase and protease inhibitors plus CPEB antibody (see Tay and Richter, 2001; Tay et al., 2003), or as a control, non-specific IgG pre-bound to magnetic beads. The CPEB-containing ribonucleoproteins were then immuno-selected and the RNA was extracted and used for RT-PCR with primers that were specific to CPE-containing RNAs. As controls, RNAs without CPEs were also analyzed (Fig. 6A). Because CPEB is present only in oocytes and not in ovarian somatic cells (Gebauer and Richter, 1996), the RNAs we detected would also be oocyte-derived. CPEB interacted with a wide range of RNAs including those that encode

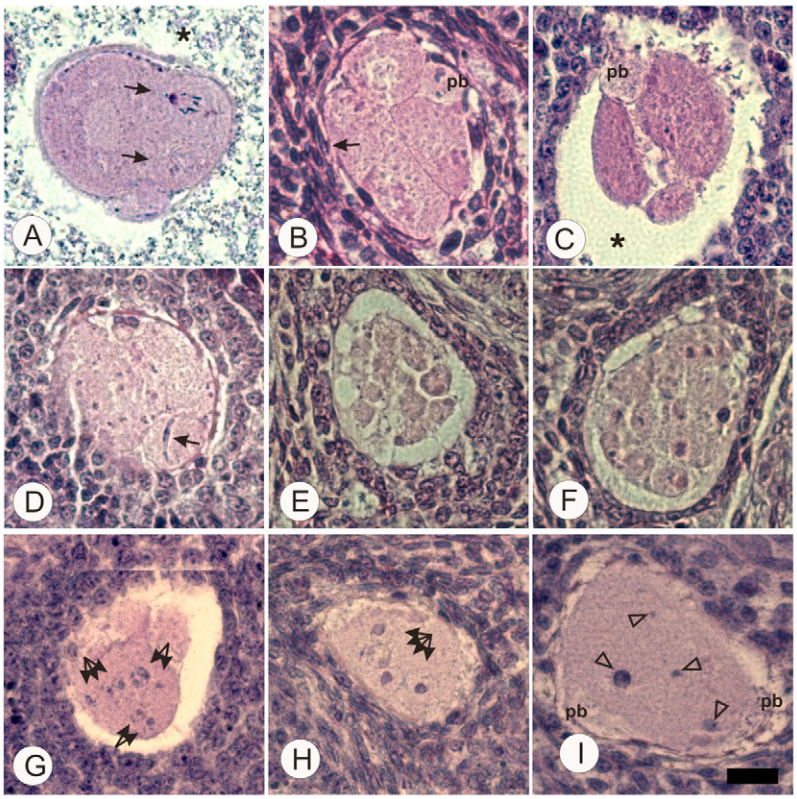

Fig. 4. Oocytes with reduced levels of CPEB undergo parthenogenetic activation. (**A**) This MI oocyte displayed two spindles and appeared to be undergoing asymmetric division with the cleavage furrow oriented longitudinally near of the spindle poles. (**B**) This four-cell embryo was enclosed in an abnormal follicle that apparently contained a polar body. The follicle contained undifferentiated and possibly apoptotic squamous granulosa cells (arrow). (**C**) This parthenote resided in an immature follicle (stage 5a-5b) and was detached from the cumulus granulosa cells. (**D**) This 7-8-cell parthenote resided in a 5a stage follicle; note the mitotic spindle in the bottom blastomere (arrow). (**E**,**F**) Multicell parthenotes enclosed in abnormal follicles (stage 4 to 5a); notice abnormally compacted granulosa cells. (**G**,**H**) Oocytes in stage 4-5b follicles with fragmented or multiple nuclei and nucleoli. (**I**) This irregularly shaped overgrown oocyte contains a number of structures in the cytoplasm that resemble nucleoli (empty arrowheads); notice two polar bodies. Scale bar: 20 μm. pb, polar bodies.

OBOX1 (Rajkovic et al., 2002) and SMAD family members (Pan et al., 2005), which are especially abundant in early oocytes (stages 2 to 4), H1FOO (Tanaka et al., 2005) and GDF9, which are abundant in primary to fully grown oocytes (stages 3b to 8), and MOS and SPIN, which are detected in fully developed oocytes (Mutter and Wolgemuth, 1987; Iwaoki et al., 1993; Oh et al., 1997). Based on these results, we think that CPEB is probably present throughout oogenesis.

CPEB interacted with mRNAs that encode proteins involved in signal transduction (e.g. *Smad1* and *Smad5*), cell cycle control (e.g. spindlin, *Bub1b*, *Mos*), transcription (e.g. *Obox1*), chromatin remodeling and regulation of gene expression (e.g. *H1foo*), maintenance of methylation patterns important for imprinting [e.g. *Dnmt1o* (*Dnmt1* – Mouse Genome Informatics)], and protein modification (*TiParp*, *Trim61*). However, we were particularly interested in *Mos* and *Gdf9* RNAs because the phenotypes associated with mice lacking these genes resemble some of the phenotypes we observed with our TG animals. For example, oocytes from *Mos* KO animals undergo parthenogenesis, as do oocytes from our TG animals. *Gdf9* KO animals exhibit granulosa cell apoptosis (when inhibin α levels are also reduced) (Wu et al., 2004) and aborted follicle development (Elvin et al., 2000); similar features were observed in our TG animals as well. We therefore examined whether the poly(A) tails of these RNAs were affected in the oocytes of TG versus wild-type animals. We initially employed a PAT [poly(A) test] described by Salles and Strickland (Salles and Strickland, 1995). This PCR-based assay was inadequate for our analysis, perhaps because of the paucity of starting material. Consequently, we employed chromatography on poly(U) Sepharose followed by thermal elution and RNA detection by RT-PCR, which has been used successfully to analyze polyadenylation of small amounts of RNA (Du and Richter, 2005). Total RNA from ovaries of 6- to 8-week-old mice (wild type and TG) was applied to the poly(U) beads, which was followed by washing and elution at increasing temperatures; RNAs with the longest tails should elute at the higher temperatures (Fig. 6B, top panel). The majority of *Mos*, *H1foo* (an oocyte-specific histone H1 variant), *Gdf9* and *Obox1* RNAs eluted at 45°C for both wild-type and TG ovaries (Fig. 6B, bottom panel); some RNA also eluted at 60°C for the wild type. These results indicate that a subpopulation of these RNAs have poly(A) tails that are shorter in the TG versus wild-type ovaries. The RNAs encoding *Mater* (*Nalp5* – Mouse Genome Informatics) and α-tubulin, which have no CPE, eluted at both temperatures in wild-type and TG ovaries. To assess whether the reduced poly(A) tail length resulted in decreased translation, a western blot for GDF9 was performed (Fig. 6C). Compared with wild type, *Gdf9* was substantially reduced in the TG ovaries. Therefore, CPEB controls the polyadenylation and translation of *Gdf9* RNA.

DISCUSSION

This study demonstrates that CPEB regulates oocyte development during the dictyate stage, and that this regulation has a profound influence on folliculogenesis as well. Because CPEB is required for meiotic progression beyond pachytene (Tay and Richter, 2001), we sought to knockdown this protein after this stage, and consequently generated *Zp3*-regulated siRNA against *Cpeb* RNA; *Zp3* is expressed only at the end of prophase I. The follicles from these transgenic animals had a range of phenotypes including premature oocyte maturation, parthenogenesis and granulosa cell apoptosis. CPEB interacted with several CPE containing RNAs, and the two encoding *Mos* and *Gdf9* had aberrantly short poly(A) tails in the TG compared with wild-type oocytes. Finally, GDF9 protein levels were markedly reduced in the TG animals, suggesting that some of the phenotypes were probably due to the paucity of this crucial growth factor.

The necessity of CPEB for oocyte growth and follicle development was an unexpected finding, which was based primarily on the CPEB phosphorylation pattern during oogenesis. CPEB T171 phosphorylation is required for cytoplasmic polyadenylation (Mendez et al., 2000a; Hodgman et al., 2001), and an analysis of mouse oocytes in prophase I showed that while this residue was phosphorylated at E16.5 (generally in pachytene), it was not at E18.5 (generally in diplotene) (Tay et al., 2003). Maturation was the next time that CPEB activity was known to occur, and at this stage it again was T171 phosphorylated. These results suggested that CPEB was not essential between pachytene and maturation. Therefore, we surmised that a knockdown of *Cpeb* after pachytene would result in maturation defects, particularly those related to *Mos* (see Introduction), the mRNA of which is translationally controlled by CPEB (Gebauer et al., 1994). However, CPEB T171 phosphorylation was not examined during the dictyate stage, so there was no a priori reason why polyadenylation-induced translation would not occur during this time. Our findings that CPEB is essential for this time of oogenesis, that it is necessary for polyadenylation and translation of (at least) *Gdf9* mRNA, suggests that it is phosphorylated during this period. We thus propose that although the phosphatase PP1 dephosphorylates CPEB at the end of prophase I, CPEB might undergo an additional phosphorylation-dephosphorylation cycle before maturation. It is also important to point out that all oocytes do not grow synchronously, but instead there are cohorts of cells at different phases of oogenesis. Thus, an analysis of ovarian oocytes from adult animals would contain oocytes at several developmental stages.

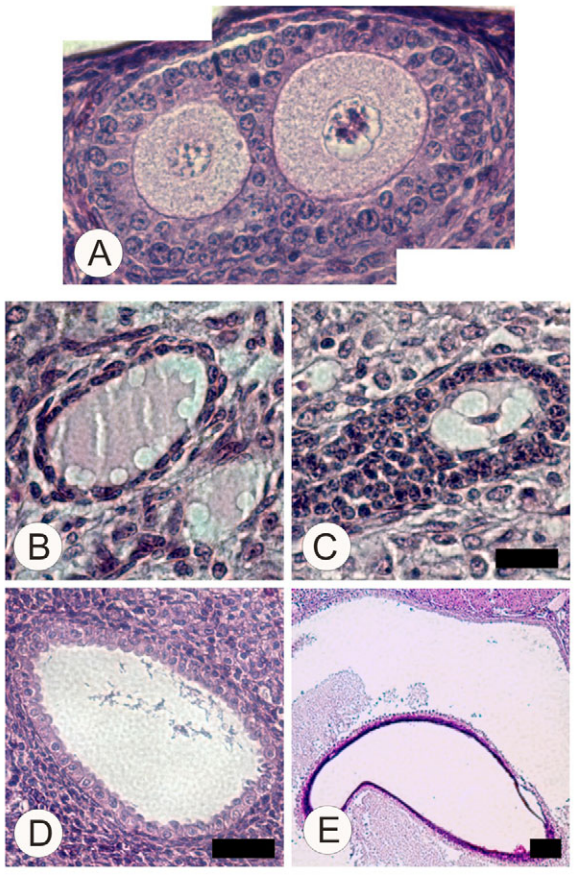

Fig. 5. *Cpeb* knockdown results in ovarian abnormalities. (**A**) This follicle contained two oocytes. (**B**) Atretic oocytes in an undifferentiated follicle composed of a single layer of the squamous granulosa cells. (**C**) This atretic follicle contained an atretic oocyte with abnormal and compacted granulosa cells (compare with Fig. 2D bottom right). (**D**,**E**) These panels show ovarian cysts in the ovaries of a 4-month-old and a 12-month-old mouse, respectively. Scale bars: 20 μm in A-C; 50 μm in D; 100 μm in E.

The range of phenotypes we observed is unlikely to be attributable to the mis-regulation of one or only a few mRNAs. Indeed, the data in Fig. 6 show that CPEB is co-immunoprecipitated with many CPE-containing RNAs. The CPE is a U-rich structure and because 3′ UTRs are often AU-rich, one might surmise that the polyadenylation and translation of many mRNAs are regulated by CPEB. An in silico analysis of 3′ UTRs revealed that up to one-third contain CPE-like sequences (Oh et al., 2000). However, 3′ UTRs can also be highly structured, which could obviate an interaction with CPEB, or contain other sequences that could inhibit polyadenylation (Simon et al., 1992). It was therefore not surprising when only about 7% of cellular RNAs were found to actually undergo cytoplasmic polyadenylation; although all the RNAs that were polyadenylated contained CPEs, some RNAs that were not polyadenylated also contained CPE-like elements (Du and Richter, 2005). While this still represents a large number of sequences, our focus on *Gdf9* mRNA as a substrate for CPEB activity during oocyte growth was suggested not only by the oocyte phenotypes in the TG animals, but by the follicle phenotypes as well. GDF9, a member of the transforming growth factor-β (TGFβ) superfamily, is synthesized in and secreted from oocytes throughout the dictyate stage (Dong et al., 1996; Elvin et al., 1999a), and is one of several proteins that coordinate oocyte and follicle development (Soyal et al., 2000; Matzuk et al., 2002). Oocytes from *Gdf9* knockout mice have an enhanced growth rate, have few surrounding granulosa cells and eventually undergo degradation/collapse/apoptosis, but occasionally undergo parthenogenetic activation in vivo and in vitro (Carabatsos et al., 1998). We have observed enhanced oocyte growth in our TG CPEB knockdown animals; these oocytes also are irregularly shaped (Fig. 4I). Several oocytes were detached from their granulosa cells and had undergone parthenogenetic activation within the ovary (Figs 3 and 4). Follicle development in *Gdf9* knockout mice is also disrupted; primary stage 3a follicles lack a thecal layer (Dong et al., 1996), and in later stage follicles granulosa cell expansion is inhibited (Elvin et al., 1999b). In the absence of GDF9 and inhibin-α, granulosa cell apoptosis occurs (Wu et al., 2004). We also detect thecal cell abnormalities and substantial granulosa cell apoptosis (Fig. 2), so it is possible that the translation of additional RNAs is reduced in the TG. Based on these observations and the fact that the poly(A) tail length of *Gdf9* RNA is reduced in the TG animals, it is not surprising that little GDF9 protein was produced. Thus, it seems probable that the lack of GDF9 (and probably others) contributes to the oocyte and follicle phenotypes in the TG animals.

In addition to *Gdf9*, *Mos* mRNA polyadenylation was also reduced in the TG mice; however, we were unable to detect MOS by immunoblotting, probably because the protein is not abundant and because of the paucity of oocytes that could be obtained from the TG ovaries. While we speculate that MOS levels may also be reduced, those few oocytes that we did obtain and culture in vitro matured normally to MII (data not shown); we did not observe any oocytes that underwent parthenogenetic activation in vitro, which was observed in the *Mos* knockout mouse (e.g. Colledge et al., 1994). It should be noted that our *Cpeb* knockdown strategy almost certainly would not result in the complete loss of CPEB in all oocytes. Indeed, some oocytes may even contain relatively normal levels of CPEB, and those may be the ones that progress normally to MII in vitro (compare Fig. 2B and Fig. S2 in the supplementary material).

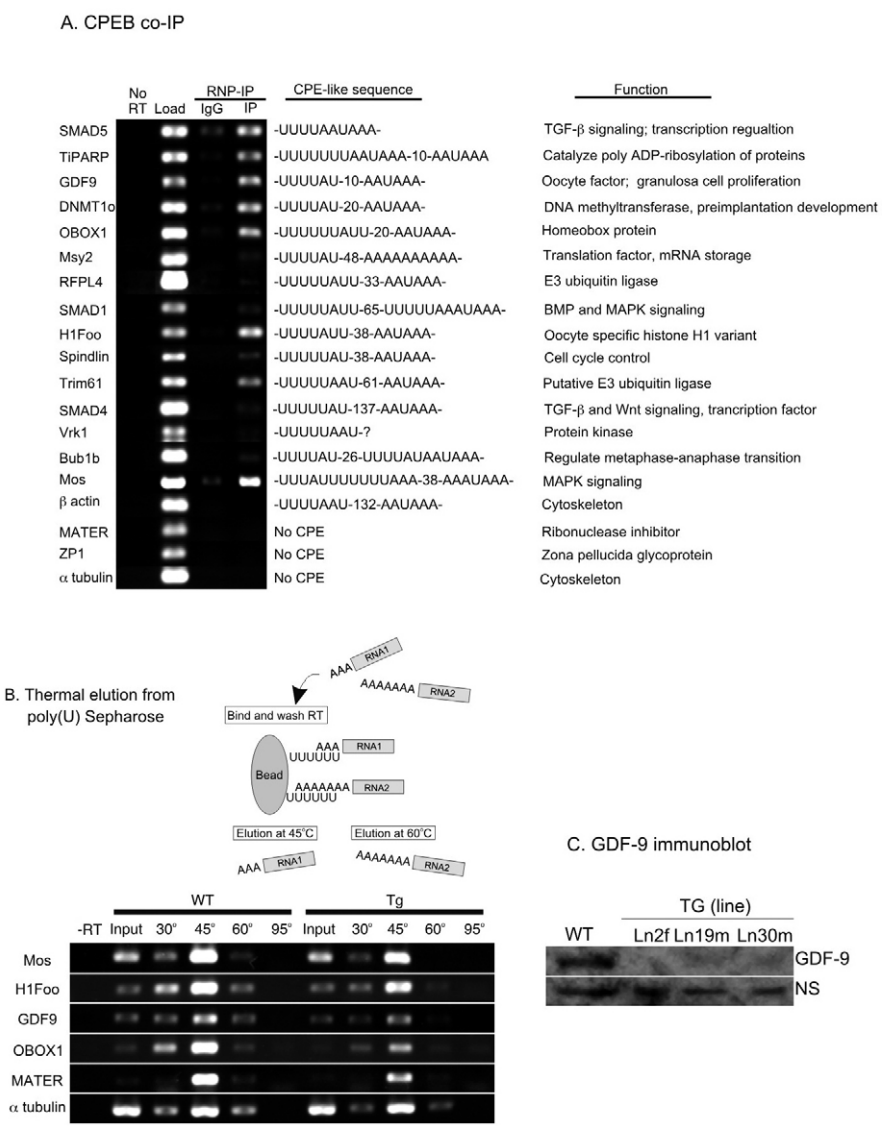

Fig. 6. RNA binding and translational control by CPEB. (**A**) Extracts from 3-week-old mice were incubated with CPEB antibody or IgG and subjected to immunoprecipitation followed by RNA extraction and RT-PCR for specific mRNAs. Two to 10% of the RNA was used for the loading control; RT refers to no reverse transcription. The sequence of the putative CPE and its distance from the AAUAAA is indicated for each RNA, as is the function of the encoded protein. (**B**) The upper panel shows the scheme of the chromatography procedure on poly (U) Sepharose followed by thermal elution. RNAs with shorter poly(A) tails elute at lower temperatures than those mRNAs with longer tails, and are detected by RT-PCR. The lower panel shows the distribution of the RT-PCR products following chromatography. In wild-type ovaries, all the RNAs eluted mostly at 45°C, but also at 60°C, indicating that the poly(A) tails were heterogeneous in length and some were long enough to elute only at the higher temperature. By contrast, all the RNAs from the TG ovaries except α-tubulin, *Zp1* and *Mater* that lack a CPE eluted completely at 45°C. These results suggest that the poly(A) tails of these RNAs were short in the TG ovaries because they eluted at a lower temperature. (**C**) Western blot shows that GDF9 (pre-processed) levels were substantially reduced in all TG lines compared with wild type. NS, a non-specific loading control.

CPEB regulation of translation is essential at least three times during oogenesis: at pachytene, during oocyte growth and during meiotic maturation. While it is not surprising that CPEB controls translation during maturation when a number of cell cycle control proteins must be synthesized, why it regulates translation at pachytene and during oocyte growth is less clear. At pachytene, CPEB regulates the polyadenylation-induced translation of *Scp1* and *Scp3* mRNAs (Tay and Richter, 2001). These mRNAs presumably are present but repressed at zygotene or even earlier; perhaps synaptonemal complex formation occurs when transcription decreases; thus, the requirement for translational activation of dormant mRNAs. Some of the target mRNAs are especially abundant in early stage oocytes (e.g. *Smad5*), while others are more abundant in fully grown oocytes (e.g. *Mos*). CPEB might orchestrate the oocyte-stage-specific translation of the class of CPE-containing mRNAs necessary for the oocyte to progress from one stage of development to the next (e.g. *Gdf9*). This succession of translation activation itself would have to be regulated by cellular cues most likely conferred by subsets of signaling cascades leading to CPEB activation/inactivation. Why mRNAs encoding a protein such as *Gdf9* would need to be regulated by CPEB during the dictyate stage is not obvious. Perhaps hormonal or other signaling cues start the cytoplasmic polyadenylation engine so that several RNAs are translated simultaneously to coordinate oocyte growth and folliculogenesis.

Because the CPE and CPEB are involved in mRNA repression as well as activation (Stutz et al., 1997; Stutz et al., 1998; de Moor and Richter, 1999; Stebbins-Boaz et al., 1999; Cao and Richter, 2002), some mRNAs in the TG oocytes might be translated preciously. Indeed, in mouse embryo fibroblasts (MEFs) derived from CPEB knockout mice, myc mRNA is translated at an elevated rate, and is involved in the bypass of cellular senescence (Groisman et al., 2006). Thus, some of the phenotypes observed in the TG oocytes could be an amalgam of underexpression and overexpression of specific mRNAs.

Finally, several of the phenotypes we observe in the *Cpeb* TG follicles resemble those of the human premature ovarian failure (POF) syndrome. POF is caused by a variety of factors (e.g. viral infections, autoimmunity, environmental toxins), including mutations in the *Gdf9* gene (Laissue et al., 2006). Because CPEB is necessary for *Gdf9* expression, it is possible that additional genetic lesions that lead to POF will map to the CPEB gene. Thus, the CPEB RNAi TG mouse described here may serve as a useful tool to elucidate some of the etiology of human POF.

We thank Richard Schultz (University of Pennsylvania), Martin Matzuk (Baylor College of Medicine) and David Garlick (Charles River Laboratories) for reagents and advice. This work was supported by a grant from the NIH (HD37267). Additional core support from the Diabetes Endocrinology Research Center Program Project (DK32520) is gratefully acknowledged.

Supplementary material

Supplementary material for this article is available at http://dev.biologists.org/cgi/content/full/133/22/4527/DC1

References

Barnard, D. C., Ryan, K., Manley, J. L. and Richter, J. D. (2004). Symplekin and xGLD-2 are required for CPEB-mediated cytoplasmic polyadenylation. *Cell* **119**, 641-651.

Barnard, D. C., Cao, Q. and Richter, J. D. (2005). Differential phosphorylation controls Maskin association with eukaryotic translation initiation factor 4E and localization on the mitotic apparatus. *Mol. Cell. Biol.* **25**, 7605-7615.

Cao, Q. and Richter, J. D. (2002). Dissolution of the maskin-eIF4E complex by cytoplasmic polyadenylation and poly(A)-binding protein controls cyclin B1 mRNA translation and oocyte maturation. *EMBO J.* **21**, 3852-3862.

Carabatsos, M. J., Elvin, J., Matzuk, M. M. and Albertini, D. F. (1998). Characterization of oocyte and follicle development in growth differentiation factor-9-deficient mice. *Dev. Biol.* **204**, 373-384.

Choi, T., Fukasawa, K., Zhou, R., Tessarollo, L., Borror, K., Resau, J. and Vande Woude, G. F. (1996). The Mos/mitogen-activated protein kinase (MAPK) pathway regulates the size and degradation of the first polar body in maturing mouse oocytes. *Proc. Natl. Acad. Sci. USA* **93**, 7032-7035.

Colledge, W. H., Carlton, M. B., Udy, G. B. and Evans, M. J. (1994). Disruption of c-mos causes parthenogenetic development of unfertilized mouse eggs. *Nature* **370**, 65-68.

de Moor, C. H. and Richter, J. D. (1999). Cytoplasmic polyadenylation elements mediate masking and unmasking of cyclin B1 mRNA. *EMBO J.* **18**, 2294-2303.

Dong, J., Albertini, D. F., Nishimori, K., Kumar, T. R., Lu, N. and Matzuk, M. M. (1996). Growth differentiation factor-9 is required during early ovarian folliculogenesis. *Nature* **383**, 531-535.

Du, L. and Richter, J. D. (2005). Activity-dependent polyadenylation in neurons. *RNA* **11**, 1340-1347.

Elvin, J. A., Clark, A. T., Wang, P., Wolfman, N. M. and Matzuk, M. M. (1999a). Paracrine actions of growth differentiation factor-9 in the mammalian ovary. *Mol. Endocrinol.* **13**, 1035-1048.

Elvin, J. A., Yan, C., Wang, P., Nishimori, K. and Matzuk, M. M. (1999b). Molecular characterization of the follicle defects in the growth differentiation factor 9-deficient ovary. *Mol. Endocrinol.* **13**, 1018-1034.

Elvin, J. A., Yan, C. and Matzuk, M. M. (2000). Oocyte-expressed TGF-beta suprfamily members in female fertility. *Mol. Cell. Endocrinol.* **159**, 1-5.

Epifano, O., Liang, L. F., Familari, M., Moos, M. C., Jr and Dean, J. (1995). Coordinate expression of the three zona pellucida genes during mouse oogenesis. *Development* **121**, 1947-1956.

Gebauer, F. and Richter, J. D. (1996). Mouse cytoplasmic polyadenylation element binding protein: an evolutionarily conserved protein that interacts with the cytoplasmic polyadenylation elements of c-mos mRNA. *Proc. Natl. Acad. Sci. USA* **93**, 14602-14607.

Gebauer, F. and Richter, J. D. (1997). Synthesis and function of Mos: the control switch of vertebrate oocyte meiosis. *Bioessays* **19**, 23-28.

Gebauer, F., Xu, W., Cooper, G. M. and Richter, J. D. (1994). Translational control by cytoplasmic polyadenylation of c-mos mRNA is necessary for oocyte maturation in the mouse. *EMBO J.* **13**, 5712-5720.

Groisman, I., Ivshina, M., Marin, V., Kennedy, N. J., Davis, R. J. and Richter, J. D. (2006). Control of cellular senescence by CPEB. *Genes Dev.* **20**, 2701-2712.

Hashimoto, N., Watanabe, N., Furuta, Y., Tamemoto, H., Sagata, N., Yokoyama, M., Okazaki, K., Nagayoshi, M., Takeda, N., Ikawa, Y. et al. (1994). Parthenogenetic activation of oocytes in c-mos-deficient mice. *Nature* **370**, 68-71.

Hodgman, R., Tay, J., Mendez, R. and Richter, J. D. (2001). CPEB phosphorylation and cytoplasmic polyadenylation are catalyzed by the kinase IAK1/Eg2 in maturing mouse oocytes. *Development* **128**, 2815-2822.

Huarte, J., Stutz, A., O'Connell, M. L., Gubler, P., Belin, D., Darrow, A. L., Strickland, S. and Vassalli, J. D. (1992). Transient translational silencing by reversible mRNA deadenylation. *Cell* **69**, 1021-1030.

Iwaoki, Y., Matsuda, H., Mutter, G. L., Watrin, F. and Wolgemuth, D. J. (1993). Differential expression of the proto-oncogenes c-abl and c-mos in developing mouse germ cells. *Exp. Cell Res.* **206**, 212-219.

Laissue, P., Christin-Maitre, S., Touraine, P., Kuttenn, F., Ritvos, O., Aittomaki, K., Bourcigaux, N., Jacquesson, L., Bouchard, P., Frydman, R. et al. (2006). Mutations and sequence variants in GDF9 and BMP15 in patients with premature ovarian failure. *Eur. J. Endocrinol.* **154**, 739-744.

Matzuk, M. M., Burns, K. H., Viveiros, M. M. and Eppig, J. J. (2002). Intercellular communication in the mammalian ovary: oocytes carry the conversation. *Science* **296**, 2178-2180.

Mendez, R. and Richter, J. D. (2001). Translational control by CPEB: a means to the end. *Nat. Rev. Mol. Cell Biol.* **2**, 521-529.

Mendez, R., Hake, L. E., Andresson, T., Littlepage, L. E., Ruderman, J. V. and Richter, J. D. (2000a). Phosphorylation of CPE binding factor by Eg2 regulates translation of c-mos mRNA. *Nature* **404**, 302-307.

Mendez, R., Murthy, K. G., Ryan, K., Manley, J. L. and Richter, J. D. (2000b). Phosphorylation of CPEB by Eg2 mediates the recruitment of CPSF into an active cytoplasmic polyadenylation complex. *Mol. Cell* **6**, 1253-1259.

Mendez R., Barnard D. and Richter J. D. (2002). Differential mRNA translation and meiotic progression require Cdc2-mediated CPEB destruction. *EMBO J.* **21**, 1833-1844.

Mutter, G. L. and Wolgemuth, D. J. (1987). Distinct developmental patterns of c-mos protooncogene expression in female and male mouse germ cells. *Proc. Natl. Acad. Sci. USA* **84**, 5301-5305.

Oh, B., Hwang, S. Y., Solter, D. and Knowles, B. B. (1997). Spindlin, a major maternal transcript expressed in the mouse during the transition from oocyte to embryo. *Development* **124**, 493-503.

Oh, B., Hwang, S., McLaughlin, J., Solter, D. and Knowles, B. B. (2000). Timely translation during the mouse oocyte-to-embryo transition. *Development* **127**, 3795-3803.

O'Keefe, S. J., Wolfes, H., Kiessling, A. A. and Cooper, G. M. (1989). Microinjection of antisense c-mos oligonucleotides prevents meiosis II in the maturing mouse egg. *Proc. Natl. Acad. Sci. USA* **86**, 7038-7042.

Pan, H., O'Brien M, J., Wigglesworth, K., Eppig, J. J. and Schultz, R. M. (2005). Transcript profiling during mouse oocyte development and the effect of gonadotropin priming and development in vitro. *Dev. Biol.* **286**, 493-506.

Pepling, M. E. and Spradling, A. C. (1998). Female mouse germ cells form synchronously dividing cysts. *Development* **125**, 3323-3328.

Pepling, M. E. and Spradling, A. C. (2001). Mouse ovarian germ cell cysts undergo programmed breakdown to form primordial follicles. *Dev. Biol.* **234**, 339-351.

Rajkovic, A., Yan, C., Yan, W., Klysik, M. and Matzuk, M. M. (2002). Obox, a family of homeobox genes preferentially expressed in germ cells. *Genomics* **79**, 711-717.

Richter, J. D. (2000). Influence of Polyadenylation-induced translation on metazoan development and neuronal synaptic function. In *Translational Control of Gene Expression* (ed. N. Sonenberg, J. Hershey and M. Mathew), pp. 785-806. Cold Spring Harbor: Cold Spring Harbor Laboratory Press.

Richter, J. D. and Sonenberg, N. (2005). Regulation of cap-dependent translation by eIF4E inhibitory proteins. *Nature* **433**, 477-480.

Roy, A. and Matzuk, M. M. (2006). Deconstructing mammalian reproduction: using knockouts to define fertility pathways. *Reproduction* **131**, 207-219.

Sagata, N. (1997). What does Mos do in oocytes and somatic cells? *Bioessays* **19**, 13-21.

Salles, F. J. and Strickland, S. (1995). Rapid and sensitive analysis of mRNA polyadenylation states by PCR. *PCR Methods Appl.* **4**, 317-321.

Sarkissian, M., Mendez, R. and Richter, J. D. (2004). Progesterone and insulin stimulation of CPEB-dependent polyadenylation is regulated by Aurora A and glycogen synthase kinase-3. *Genes Dev.* **18**, 48-61.

Simon, R., Tassan, J. P. and Richter, J. D. (1992). Translational control by poly(A) elongation during *Xenopus* development: differential repression and enhancement by a novel cytoplasmic polyadenylation element. *Genes Dev.* **6**, 2580-2591.

Simon, R., Wu, L. and Richter, J. D. (1996). Cytoplasmic polyadenylation of activin receptor mRNA and the control of pattern formation in Xenopus development. *Dev. Biol.* **179**, 239-250.

Soyal, S. M., Amleh, A. and Dean, J. (2000). FIGalpha, a germ cell-specific transcription factor required for ovarian follicle formation. *Development* **127**, 4645-4654.

Stebbins-Boaz, B., Cao, Q., de Moor, C. H., Mendez, R. and Richter, J. D. (1999). Maskin is a CPEB-associated factor that transiently interacts with eIF-4E. *Mol. Cell* **4**, 1017-1027.

Stein, P., Svoboda, P. and Schultz, R. M. (2003). Transgenic RNAi in mouse oocytes: a simple and fast approach to study gene function. *Dev. Biol.* **256**, 187-193.

Stutz, A., Huarte, J., Gubler, P., Conne, B., Belin, D. and Vassalli, J. D. (1997). In vivo antisense oligodeoxynucleotide mapping reveals masked regulatory elements in an mRNA dormant in mouse oocytes. *Mol. Cell. Biol.* **17**, 1759-1767.

Stutz, A., Conne, B., Huarte, J., Gubler, P., Volkel, V., Flandin, P. and Vassalli, J. D. (1998). Masking, unmasking, and regulated polyadenylation cooperate in the translational control of a dormant mRNA in mouse oocytes. *Genes Dev.* **12**, 2535-2548.

Svoboda, P., Stein, P. and Schultz, R. M. (2001). RNAi in mouse oocytes and preimplantation embryos: effectiveness of hairpin dsRNA. *Biochem. Biophys. Res. Commun.* **287**, 1099-1104.

Tanaka, M., Kihara, M., Hennebold, J. D., Eppig, J. J., Viveiros, M. M., Emery, B. R., Carrell, D. T., Kirkman, N. J., Meczekalski, B., Zhou, J. et al.

(2005). H1FOO is coupled to the initiation of oocytic growth. *Biol. Reprod.* **72**, 135-142.

Tay, J. and Richter, J. D. (2001). Germ cell differentiation and synaptonemal complex formation are disrupted in CPEB knockout mice. *Dev. Cell* **1**, 201-213.

Tay, J., Hodgman, R. and Richter, J. D. (2000). The control of cyclin B1 mRNA translation during mouse oocyte maturation. *Dev. Biol.* **221**, 1-9.

Tay, J., Hodgman, R., Sarkissian, M. and Richter, J. D. (2003). Regulated CPEB phosphorylation during meiotic progression suggests a mechanism for temporal control of maternal mRNA translation. *Genes Dev.* **17**, 1457-1462.

Tenenbaum S. A., Carson C. C., Lager P. J. and Keene J. D. (2000). Identifying mRNA subsets in messenger ribonucleoprotein complexes by using cDNA arrays. *Proc. Natl. Acad. Sci. USA* **97**, 14085-14090.

Tunquist, B. J. and Maller, J. L. (2003). Under arrest: cytostatic factor (CSF)-mediated metaphase arrest in vertebrate eggs. *Genes Dev.* **17**, 683-710.

Vassalli, J. D., Huarte, J., Belin, D., Gubler, P., Vassalli, A., O'Connell, M. L., Parton, L. A., Rickles, R. J. and Strickland, S. (1989). Regulated polyadenylation controls mRNA translation during meiotic maturation of mouse oocytes. *Genes Dev.* **3**, 2163-2171.

Wickens, M., Goodwin, E. B., Kimble, J., Strickland, S. and Hentze, M. (2000). Translational control of developmental decisions. In *Translational Control of Gene Expression* (ed. N. Sonenberg, J. Hershey and M. Mathews), pp. 295-370. Cold Spring Harbor: Cold Spring Harbor Laboratory Press.

Wu, X., Chen, L., Brown, C. A., Yan, C. and Matzuk, M. M. (2004). Interrelationship of growth differentiation factor 9 and inhibin in early folliculogenesis and ovarian tumorigenesis in mice. *Mol. Endocrinol.* **18**, 1509-1519.